Journal of the Geological Society

Effects of melt percolation on platinum group elements and Re–Os systematics of peridotites from the Tan-Lu fault zone, eastern North China Craton

Yan Xiao and Hong-Fu Zhang

Journal of the Geological Society 2011; v. 168; p. 1201-1214
doi: 10.1144/0016-76492010-113

Journal of the Geological Society, London, Vol. **168**, 2011, pp. 1201–1214. doi: 10.1144/0016-76492010-113.

Effects of melt percolation on platinum group elements and Re–Os systematics of peridotites from the Tan-Lu fault zone, eastern North China Craton

YAN XIAO* & HONG-FU ZHANG

State Key Laboratory of Lithospheric Evolution, Institute of Geology and Geophysics, Chinese Academy of Sciences, PO Box 9825, Beijing 10029, China

**Corresponding author (e-mail: xiaoyan@mail.iggcas.ac.cn)*

Abstract: Concentrations of platinum group elements (PGE) and Re–Os isotopic compositions were determined for a suite of peridotite xenoliths from Cenozoic Beiyan volcanoes within the Tan-Lu fault zone, eastern North China Craton (NCC). Previous petrographic and geochemical data indicate the existence of considerable modification by melt–peridotite interaction for these xenoliths. Thus, this suite of xenoliths provides an unusual opportunity to examine the effects of melt percolation on PGE abundances and Re–Os isotopes. Our data show that most of the Beiyan peridotites have flat chondrite-normalized PGE patterns whereas a considerable variation in total PGE abundances has been observed in lherzolites to highly fertile cpx-rich lherzolites and wehrlites. Their total PGE contents range between 0.97 and 61.4 ppb and their PGE relative abundances from 0.1 to 0.0001 × CI-chondrites, respectively. In these rocks, the total PGE budget was reduced by more than 90% from lherzolite to cpx-rich lherzolite and to wehrlite, probably because intergranular sulphides were completely removed by silicate melt. However, Beiyan peridotites have low and variable Re (0.0002–0.5118 ppb) and Os (0.194–10.4 ppb) abundances and high $^{187}Os/^{188}Os$ (0.12167–0.14978) ratios. The $^{187}Os/^{188}Os$ ratios in some wehrlites are much higher than the value for the primitive mantle. The high $^{187}Os/^{188}Os$ ratios have also been observed in peridotites found in other localities within the Tan-Lu fault zone such as Shanwang and Nüshan. This could be the result of the addition of radiogenic Os during the melt percolation. Extremely low Os abundances in Beiyan peridotites suggest that Os may behave as an incompatible element during melt percolation and could mobilize with the dissolution of sulphides. The suprachondritic $^{187}Os/^{188}Os$ ratios in peridotites within the Tan-Lu fault zone relative to those away from it indicate that the Tan-Lu fault zone played an important role as a melt infiltrating channel in the radiogenic Os enrichment induced by melt percolation. This could be the reason for the Os isotopic heterogeneity observed in the eastern NCC. This study also confirms that Os isotopes and PGE appear to be mobile during massive melt percolation.

Archaean cratons are underlain by mantle lithosphere with a high viscosity (Kelemen *et al.* 1998; Griffin *et al.* 1999). Such lithosphere is thick, cold and refractory, and thus contributes significantly to craton stability. However, asthenosphere–lithosphere and crust–mantle interactions can modify ancient lithospheric mantle roots by the influx of fertile materials (Kelemen *et al.* 1998; Bedini *et al.* 1997; Bedini & Bodinier 1999; Griffin *et al.* 1998; Downes 2001; Rudnick *et al.* 2004; Zhang 2005; Zheng *et al.* 2005; Zhang *et al.* 2009*a*). Mantle xenoliths are direct samples of lithospheric mantle fragments, and thus can provide direct information about these mantle processes.

The North China Craton (NCC) is one of the major Archaean cratons in eastern Eurasia with crustal remnants as old as 3.8 Ga (Liu *et al.* 1992) (Fig. 1a). It had a cold (*c.* 40 mW m^{-2}), thick (*c.* 200 km) and refractory lithosphere during the early Palaeozoic, as inferred from peridotite xenoliths, xenocryst minerals, and diamond inclusions in Mid-Ordovician diamondiferous kimberlites (Menzies *et al.* 1993, 2007; Harris *et al.* 1994; Meyer *et al.* 1994; Zheng *et al.* 1998, 2001, 2007; Zhang & Yang 2007). However, peridotite xenoliths derived from the late Mesozoic and Cenozoic basalts from the NCC suggest a relatively hot, thin and fertile lithosphere beneath the eastern NCC (Menzies *et al.* 1993; Griffin *et al.* 1998; Fan *et al.* 2000; Xu 2001; Zheng *et al.* 2001; Rudnick *et al.* 2004; Ying *et al.* 2006; Tang *et al.* 2008; Zhang *et al.* 2009*b*). They also have an ‘oceanic’ affinity (Boyd 1989; Fan *et al.* 2000). This implies that the lithospheric mantle of the NCC has not only been considerably thinned but also been compositionally changed from highly refractory to more fertile mantle during Phanerozoic times. Additionally, studies on mantle olivine xenocrysts and peridotite xenoliths from the late Mesozoic–Cenozoic basalts show that many suites of xenoliths more or less underwent melt–peridotite interaction in Mesozoic and Cenozoic times (Zhang 2005; Ying *et al.* 2006; Tang *et al.* 2008; Zhang *et al.* 2009*a*,*b*; Xiao *et al.* 2010). However, the scale of melt–peridotite interaction and character of the melt remain unclear.

The platinum group elements (PGE) comprise osmium (Os), iridium (Ir), ruthenium (Ru), rhodium (Rh), platinum (Pt), and palladium (Pd). Rhenium (Re) is often discussed along with the PGE because of its similar geochemical behaviour and component part of Re–Os isotope decay system. Abundances of PGE and Re and $^{187}Os/^{188}Os$ isotopes in the bulk mantle xenoliths can potentially provide important information about the processes of earth accretion, core–mantle segregation, and mantle differentiation (Lorand *et al.* 1993; Pattou *et al.* 1996; Rehkämper *et al.* 1997; Snow & Schmidt 1998; Handler & Bennett 1999; Morgan *et al.* 2001). Additionally, PGE and Re–Os isotopic systematics of single mantle rocks have been given increasing attention recently because they commonly record complex histories of smaller-scale processes such as melt depletion, melt percolation, and mantle metasomatism (Handler *et al.* 1999; Rehkämper *et al.* 1999; Becker *et al.* 2001; Lorand

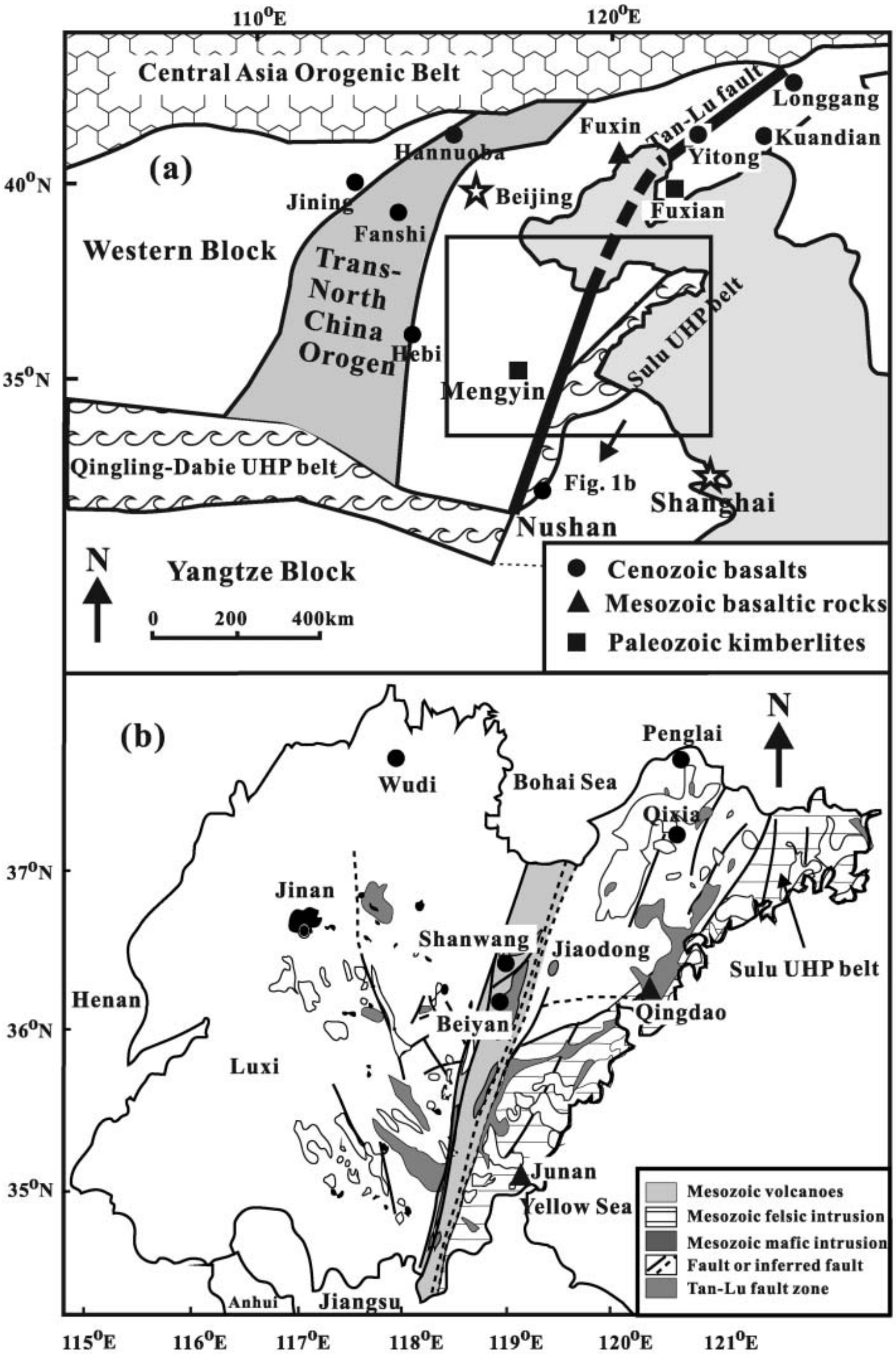

Fig. 1. Simplified geological map showing major tectonic units of the NCC and the xenolith localities mentioned in the text. (**a**) The tectonic subdivisions of the NCC (after Zhao *et al.* 2001). (**b**) Distribution of Mesozoic intrusions and volcanic rocks in Shandong Province, as well as Palaeozoic Mengyin diamondiferous kimberlite, with emphasis on basalts and related rocks (after Zhang & Sun 2002).

& Alard 2001; Büchl *et al.* 2002, 2004; Lee 2002; Chesley *et al.* 2004; Lorand *et al.* 2004; Pearson *et al.* 2004; Reisberg *et al.* 2005; Ionov *et al.* 2006; Ackerman *et al.* 2009; Zhang *et al.* 2009*a*). Such processes tend to obscure the primary PGE characteristics of the bulk mantle, but can provide useful information about regional and local processes. For example, Re is a moderately incompatible element, whereas Os is a strongly compatible element (Shirey & Walker 1998). Partial melting imparts a strong parent–daughter fractionation to the residual peridotite and Os is not easily overprinted by metasomatism. Thus the Re–Os isotope system has the greatest potential to date melt depletion events in peridotites (Walker *et al.* 1989). Recent studies also show that metasomatic processes including melt/fluid infiltration and percolation can also significantly alter absolute and relative PGE concentrations and affect Re–Os dating in mantle peridotites (Lorand *et al.* 2003, 2004, 2008; Reisberg *et al.* 2005; Becker *et al.* 2006; Ackerman *et al.* 2009; Rudnick & Walker 2009; Zhang *et al.* 2009*a*). Despite considerable studies of the behaviour of PGE and Re–Os resulting from different types and extents of metasomatic processing, the mechanism of metasomatism affecting them is still obscure.

Here, we present PGE–Re data, as well as $^{187}Os/^{188}Os$ isotopic compositions of well-characterized and variably (but typically strongly) metasomatized peridotite xenoliths from the eastern NCC with the aim of addressing the behaviour of PGE, Re and $^{187}Os/^{188}Os$ in peridotites during massive melt percolation. In addition, previously published PGE and $^{187}Os/^{188}Os$ data for mantle xenoliths from the NCC (Xu *et al.* 1998*b*; Gao *et al.* 2002; Wu *et al.* 2003, 2006; Zhang *et al.* 2007, 2008, 2009*a*; Zhi *et al.* 2007; Chu *et al.* 2009; Liu *et al.* 2010; Zhou *et al.* 2010) have been incorporated for comparison in order to constrain the origin of Os isotope heterogeneity and the evolution of lithospheric mantle on a regional scale beneath the NCC.

Geological setting and sample description

The xenoliths in this study are from Cenozoic alkali basalts at Beiyan within the Tan-Lu fault zone, eastern NCC (Fig. 1b). These xenoliths show few effects of surface alteration and are large (10–15 cm). Mineral major and trace element data and Sr–Nd isotopic compositions have previously been reported for these xenoliths (Xiao *et al.* 2010).

Three main rock types have been identified among the Beiyan peridotite xenoliths (Xiao *et al.* 2010): lherzolite, cpx-rich lherzolite and wehrlite. Lherzolites are characterized by low forsterite contents (Fo 89–91) in olivines and spoon-shaped to slightly light REE (LREE)-enriched patterns, reflecting recent metasomatic overprinting (Fig. 2a). They represent fragments of newly accreted lithospheric mantle that makes up part of the Late Mesozoic–Cenozoic lithosphere beneath the eastern NCC (Zheng *et al.* 1998, 2007; Ying *et al.* 2006; Chu *et al.* 2009; Zhang *et al.* 2009*b*, 2010). Cpx-rich lherzolites and wehrlites are strongly metasomatized, as indicated by convex-upward trace element patterns and the presence of accessory minerals (alkali feldspar, phlogopite, calcite and amphibole) (Fig. 2a and b). They were produced by the interaction of lherzolites with evolved carbonatitic silicate melts, which partially or completely replaced opx with cpx and caused moderate to strong Fe enrichment (Xiao *et al.* 2010).

Analytical methods

Major element analyses

Whole rocks were powdered with an agate mill to 200 mesh and 6 g powders were weighed. Major element analyses were determined by X-ray fluorescence spectrometry (XRF) using a Phillips PW 2400 sequential XRF instrument at the Institute of Geology and Geophysics (IGG), Chinese Academy of Sciences. The analytical precision is better than ±2% for major oxides. The results are given in Table 1.

PGE and Re–Os isotopic measurements

Each of the sample powders (15 g) was weighed into a fire-clay crucible, mixed with 40 g $Na_2B_4O_7$, 2.5 g Fe, 1.0 g Ni and 1.0 g S. Appropriate amounts of ^{185}Re and ^{190}Os spike solutions were then added to the mixture. The mixture was covered and fused at 1050 °C for 45 min. A sulphide bead was recovered and placed in a glass beaker containing 15 ml H_2O. After the bead disintegrated into powder, 30 ml of HCl were added. On heating, the solution became clear and then was filtered to collect insoluble residue. The residue was transferred into a distillation apparatus with 3 ml HNO_3 and then distilled for Os, which was absorbed with 5 ml H_2O for inductively coupled plasma mass spectrometry (ICP-MS) determination or 5 ml HBr for negative thermal ionization mass spectrometry (N-TIMS) analysis. After distillation, the remaining solution was concentrated and made up to 10 ml with 2% aqua regia for analysis of Ru, Rh, Pd, Re, Ir and Pt by an Elan6000 ICP-MS system (PerkinElmer) at the Guangzhou Institute of Geochemistry, Chinese Academy of Sciences (Sun *et al.* 2009). Os in the HBr solution was further purified using the micro-distillation method and was analysed with an IsoProbe-T (ThermElectron) at IGG, Chinese Academy of Sciences (Chu *et al.* 2009).

Results

Whole-rock major element variations

Beiyan peridotites show a considerable variation in major element compositions, ranging from fertile compositions similar to those of lherzolites from the NCC such as those at Hannuoba, Fanshi, Kuandian, Penglai (Wu *et al.* 2003; Rudnick *et al.* 2004; Tang *et al.* 2008; Chu *et al.* 2009; Zhang *et al.* 2009*a*) to highly fertile cpx-rich lherzolite and wehrlites similar to the Shanwang, Nüshan and Yitong peridotites within the Tan-Lu fault zone (Zheng *et al.* 1998; Chu *et al.* 2009; Liu *et al.* 2010; Xiao *et al.* 2010; Zhou *et al.* 2010). Most lherzolites plot within the compositional field of peridotites from the Tan-Lu fault zone, different from the cratonic peridotites (Fig. 3). At Beiyan, the CaO content increases from lherzolites (2.12–3.88 wt%) to

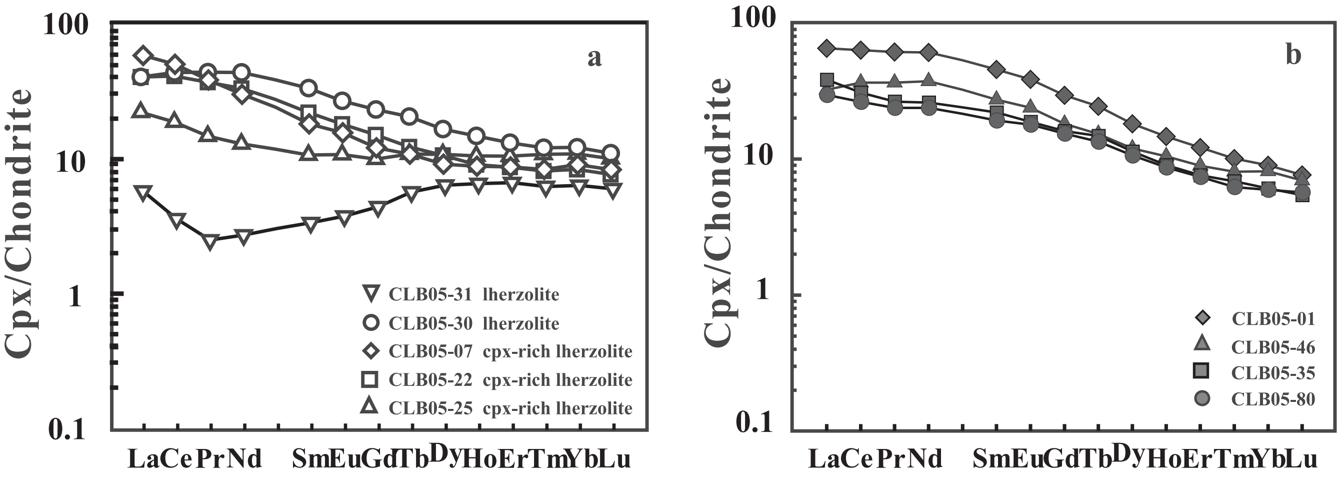

Fig. 2. Chondrite-normalized REE patterns of cpx from the Beiyan xenoliths. The cpx data are from Xiao *et al.* (2010) and the normalizing values are after McDonough & Sun (1995).

Table 1. *Major oxides of mantle xenoliths entrained in Beiyan basalts (wt%)*

Rock:	Lherzolite						Cpx-rich lherzolite				Wehrlite			
Sample:	CLB05-03	CLB05-24	CLB05-30	CLB05-31	CLB05-48	CLB05-50	CLB05-07	CLB05-22	CLB05-25	CLB05-53	CLB05-01	CLB05-35	CLB05-46	CLB05-80
SiO_2	43.0	43.4	44.8	45.4	44.4	44.4	42.3	44.4	43.7	43.4	42.4	37.8	42.9	40.6
TiO_2	0.05	0.01	0.33	0.03	0.07	0.09	0.11	0.05	0.17	0.07	0.12	0.49	0.17	0.44
Al_2O_3	1.32	0.74	4.28	2.31	3.43	3.12	2.37	2.14	3.66	2.45	1.30	4.23	2.17	3.19
$Fe_2O_3{}^T$	11.5	8.75	10.0	7.95	9.01	9.43	10.7	10.0	11.8	9.82	11.2	14.8	10.5	14.8
MnO	0.14	0.13	0.15	0.11	0.13	0.13	0.21	0.14	0.16	0.14	0.17	0.19	0.15	0.17
MgO	41.3	40.8	34.5	39.6	38.3	39.7	35.2	40.0	35.7	41.3	39.9	29.5	38.8	35.1
CaO	2.12	2.40	3.88	2.90	3.06	2.48	4.54	2.38	3.58	2.20	2.57	7.64	3.32	4.51
Na_2O	0.16	0.03	0.49	0.18	0.31	0.27	0.40	0.29	0.43	0.22	0.21	0.26	0.28	0.32
K_2O	0.02	0.05	0.22	0.04	0.03	0.03	0.19	0.02	0.06	0.05	0.14	0.11	0.10	0.11
P_2O_5	0.02	0.02	0.05	0.01	0.01	0.02	0.43	0.02	0.04	0.04	0.05	0.09	0.05	0.06
LOI	0.56	3.38	1.64	1.54	1.32	0.54	3.24	0.80	0.62	0.78	1.88	4.85	1.52	1.08
Total	100.2	99.7	100.3	100.1	100.1	100.2	99.8	100	99.9	100.5	99.9	99.9	99.9	100.4
FeO	8.69	6.08	7.14	6.35	6.88	7.29	7.71	7.64	8.78	7.43	8.32	9.70	7.87	10.7
Mg-no.	89.5	92.4	89.7	91.8	90.9	90.8	89.2	90.4	88.0	90.9	89.6	84.6	89.9	89.6

LOI, loss on ignition. Mg-number = $Mg/(Mg + Fe^{2+}) \times 100$. $Fe_2O_3{}^T$ represents total Fe.

cpx-rich lherzolites (2.20–4.54 wt%) and wehrlites (2.57–7.64 wt%) accompanied by a decrease in MgO (Fig. 3a). Some cpx-rich lherzolites and wehrlites have somewhat higher CaO than primitive mantle, which might have resulted from later addition of Ca-rich cpx, and show a trend with other lherzolites (Fig. 3a). The Al_2O_3 contents of lherzolite (0.74–4.28 wt%), cpx-rich lherzolite (0.74–2.45 wt%) and wehrlite (1.3–4.23 wt%) overlap, but Beiyan cpx-rich lherzolite and wehrlites deviate from the field of lherzolites (Fig. 3b).

PGE concentrations

Nine Beiyan xenoliths show a broader PGE concentration range of 0.19–10.4 ppb for Os, 0.13–9.06 ppb for Ir, 0.25–14.6 ppb for Ru, 0.04–2.93 ppb for Rh, 0.21–13.4 ppb for Pt, and 0.15–11.0 ppb for Pd (Table 2). This is identical to the compositional range reported for other basalt-hosted spinel peridotites worldwide (e.g. Morgan 1986; Handler *et al.* 1997, 1999; Rehkämper *et al.* 1997; Lorand & Alard 2001; Meisel *et al.* 2001; Lorand *et al.* 2003; Ionov *et al.* 2006; Ackerman *et al.* 2009). The Beiyan peridotites display considerable sample-to-sample variations in PGE abundances that exceed the external reproducibility of each element. Most Beiyan peridotites broadly have flat chondrite-normalized PGE patterns with slight depletion in Pt, except for one wehrlite (CLB05-01), which is depleted in Pd (Fig. 4). Two wehrlites (CLB05-80 and CLB05-35) with the lowest MgO contents have extremely low values for all the PGE (total PGE 0.97–1.94 ppb). Os, Ru, Rh, Pt and Pd are positively correlated with Ir in the Beiyan peridotites (Fig. 5) although their PGE abundances are much lower than the value of the primitive mantle, except for one sample (CLB05-31) with the highest Fo. Furthermore, none of the PGE positively correlate with Al_2O_3 and CaO (not shown).

Most Beiyan peridotites have roughly chondritic Pd/Ir ratios (0.88–1.07) whereas two lherzolites (CLB05-07 and CLB05-25) show subchondritic Pd/Ir ratios (0.43). One wehrlite (CLB05-01) has an extremely low Pd/Ir ratio of 0.07, probably reflecting that those PGE form alloys or discrete platinum group metals (PGM), such as Pt–Pd–Os–Ir (Lorand & Alard 2010). Another wehrlite (CLB05-46) has a suprachondritic Pd/Ir ratio of 1.73. All the Beiyan peridotites, excluding the wehrlite CLB05-01, show chondritic Os/Ir ratios and suprachondritic Pd/Pt ratios.

In addition, Beiyan peridotites show a considerable range in total PGE concentrations (61.35–0.97 ppb), from fertile lherzolites similar to other lherzolites such as those at Shanwang, Nüshan and Yitong within the Tan-Lu fault zone (Chu *et al.* 2009; Liu *et al.* 2010; Zhou *et al.* 2010) to highly fertile cpx-rich lherzolites and wehrlites with decreasing MgO (Fig. 6a). The compatible element Ni contents in these Beiyan xenoliths are much lower than those of basalt-hosted xenoliths suites worldwide (McDonough & Sun 1995; Chu *et al.* 2009) (Fig. 6b and c). The incompatible element Cu contents relative to PGE for Beiyan peridotites show a broader range (3.52–54.6 ppm), similar to those from the eastern NCC (Chu *et al.* 2009).

Re–Os isotopic systematics

Re and Os concentrations and Re–Os isotopic ratios are listed in Table 3. The Os abundances range from 0.19 to 3.54 ppb, except for sample CLB05-31, which may contain as much as 10.4 ppb Os. This concentration range is similar to that reported for peridotite xenoliths from the basalts in the NCC (Gao *et al.* 2002; Wu *et al.* 2003, 2006; Zhi *et al.* 2007; Chu *et al.* 2009;

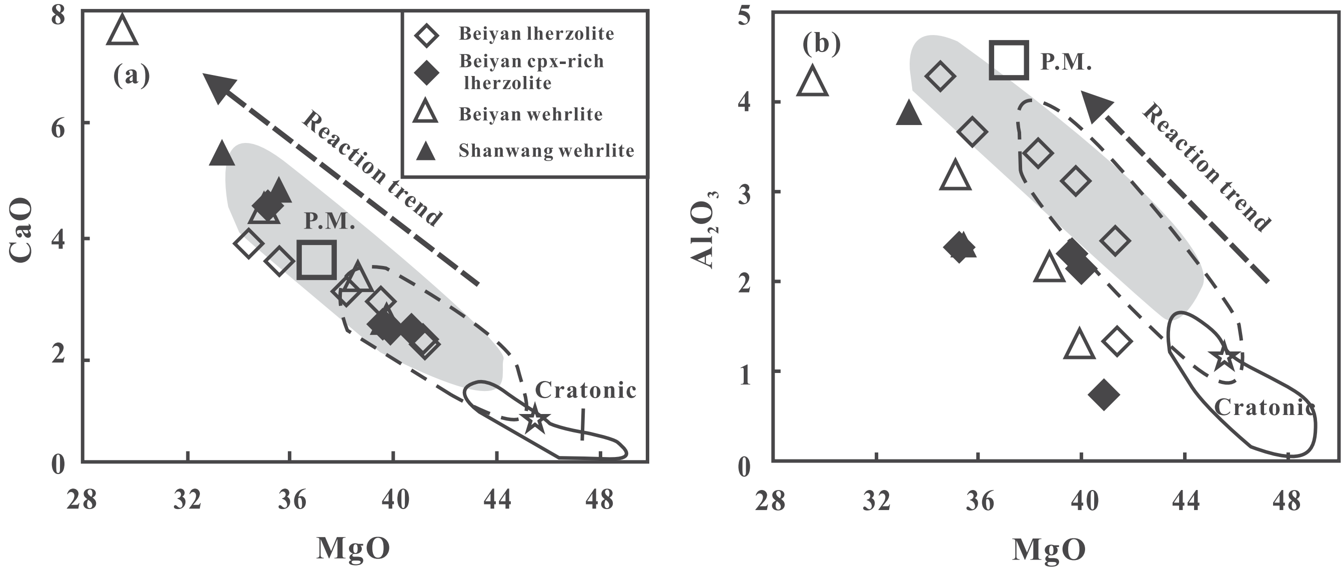

Fig. 3. Major element variations for Beiyan peridotite xenoliths. P.M., primitive mantle (McDonough & Sun 1995). Continuous-line field indicates cratonic peridotites (Tanzanian xenoliths; Lee & Rudnick 1999). Star indicates average peridotitic xenoliths from the Arkaean (Griffin *et al.* 1999). Dashed-line field represents peridotites from Hannuoba (Gao *et al.* 2002; Zhang *et al.* 2009*a*), Longgang (Wu *et al.* 2003), Kuandian (Wu *et al.* 2006), Penglai (Chu *et al.* 2009) and Qixia (Gao *et al.* 2002). Grey shaded field indicates Shanwang lherzolites and Nüshan peridotites within the Tan-Lu fault zone (Zhi *et al.* 2007; Chu *et al.* 2009; Liu *et al.* 2010; Zhou *et al.* 2010).

Table 2. *PGE compositions of Beiyan peridotites*

Sample	Os (ppb)	Ir (ppb)	Ru (ppb)	Rh (ppb)	Pt (ppb)	Pd (ppb)	Total (ppb)	Ni (ppm)	Cu (ppm)	$(Pd/Ir)_N$
Lherzolite										
CLB05-30	0.92	0.62	1.73	0.23	0.79	0.78	5.01	1694	3.52	1.04
CLB05-31	10.4	9.06	14.6	2.93	13.4	11.0	61.4	1375	25.1	1.01
Cpx-rich lherzolite										
CLB05-07	0.95	0.72	1.56	0.19	0.77	0.37	4.56	1445	4.94	0.43
CLB05-22	3.54	2.89	5.12	0.88	4.16	3.39	20.0	1811	14.3	0.97
CLB05-25	0.42	0.46	1.81	0.30	0.27	0.24	3.50	1072	9.59	0.43
Wehrlite										
CLB05-01	2.32	2.08	5.98	0.57	2.23	0.18	13.4	1714	20.5	0.07
CLB05-35	0.19	0.13	0.25	0.04	0.21	0.15	0.97	1038	34.8	0.95
CLB05-46	3.21	2.32	5.07	0.82	4.06	4.85	20.3	1663	11.0	1.72
CLB05-80	0.31	0.27	0.50	0.09	0.48	0.29	1.94	1286	54.6	0.89

The subscript N denotes the chondrite-normalized element ratio (Anders & Grevesse 1989).

Zhang *et al.* 2009*a*) although Os values in Beiyan wehrlites (CLB05-35 and CLB05-80) are very low.

Re concentrations vary from 0.03 to 0.51 ppb, except for one sample (CLB05-07), which has an exceedingly low Re (0.0002 ppb). In particular, Beiyan peridotites have much lower Re abundances than the estimated primitive mantle value (0.28 ppb) (McDonough & Sun 1995), except for sample CLB05-31. Re abundances in Beiyan wehrlites overlap with those in lherzolite xenoliths of the NCC. Overall, although Re and Os abundances in the Beiyan xenoliths do not correlate (Fig. 7), Os decreases with decreasing MgO, as in other suites of the eastern NCC (Fig. 8).

Beiyan peridotites have carbonaceous chondritic (0.127; after Shirey & Walker 1998) to suprachondritic $^{187}Os/^{188}Os$ ratios (0.12167–0.14978), slightly higher than those from the eastern NCC (Wu *et al.* 2003, 2006; Zhi *et al.* 2007; Zhang *et al.* 2008, 2009*a*; Chu *et al.* 2009; Liu *et al.* 2010; Zhou *et al.* 2010) (Fig. 9). The Beiyan peridotites with high $^{187}Os/^{188}Os$ ratios have low Os concentrations (Fig. 10), suggesting a mixing trend between peridotite and components with radiogenic Os and low Os concentrations.

Discussion

Behaviour of the PGE in mantle processes (partial melting and metasomatism)

The distribution of PGE in the upper mantle is largely controlled by base metal sulphides (BMS; monosulphide solid solution (Mss), pyrrhotite, pentlandite, chalcopyrite) resulting from extremely high ($>10^3$) sulphide/silicate melt partition coefficients (Mitchell & Keays 1981; Pattou *et al.* 1996; Alard *et al.* 2000; Lorand & Alard 2001; Luguet *et al.* 2004). The PGE are also partially hosted by platinum-group minerals (PGM) and PGE-bearing alloys in some mantle rocks (Luguet *et al.* 2007; Lorand & Alard 2010). Experiments and *in situ* analytical data for

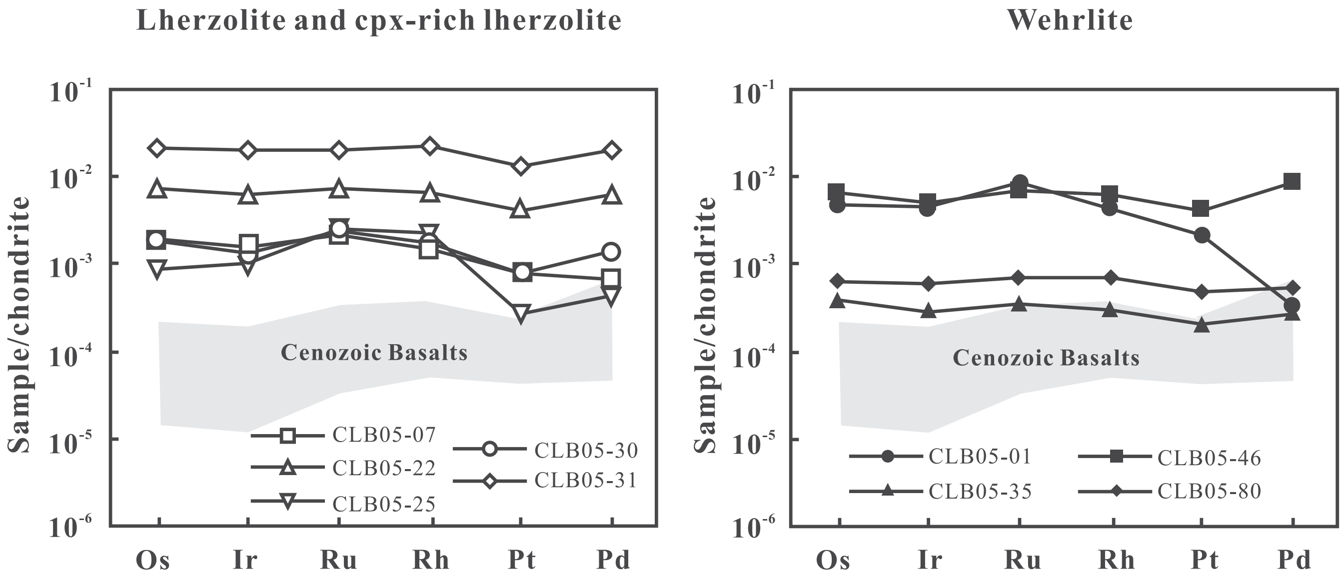

Fig. 4. Chondrite-normalized HFSE patterns of Beiyan lherzolites and wehrlites. Chondrite normalizing values are after Fischer-Gödde *et al.* (2010). Grey shaded field indicates the Cenozoic basalts from Jining (W.H. Zhang, unpublished data).

sulphides in mantle rocks indicate that Mss preferentially accommodates I-PGE (Os, Ir, Ru) relative to Cu-rich sulphides, which concentrate P-PGE (Rh, Pt, Pd) (Lorand *et al.* 1999; Alard *et al.* 2000; Lorand & Alard 2001; Luguet *et al.* 2004). Once mantle rocks underwent melt depletion, Cu-rich sulphides could be dissolved prior to Mss (Bockrath *et al.* 2004), resulting in fractionation of P-PGE from I-PGE. This results in a decrease of P-PGE/I-PGE ratios such as Pd/Ir with progressive melting, whereas I-PGE is generally little affected by partial melting.

The lithospheric mantle beneath Beiyan experienced low degrees of partial melting (Xiao *et al.* 2010). Most Beiyan peridotites carry a chondrite-like PGE signature and the PGE do not show clear correlation with indices of fertility such as CaO (not shown). Additionally, very high degrees of partial melting (⩾25%) would be necessary to generate the low Pd/Ir ratios found in sample CLB05-01. Such a high degree of partial melting is inconsistent with major and trace element data (Xiao *et al.* 2010). This may imply that the distribution of Pd was controlled by a different trace phase than the other PGE, and that this phase was more greatly affected by melt percolation than the phases controlling the other PGE. Furthermore, this sample with low Al_2O_3 (1.3%) may not reflect the refractory residue of partial melting, but may have been disturbed by an aluminium-poor metasomatic component such as a carbonatitic silicate melt. Therefore, the Al_2O_3 contents of Beiyan peridotites have not been considered as a robust partial melting index. Thus, we conclude that partial melting was not the dominant process controlling PGE abundances of Beiyan peridotites.

On the other hand, metasomatic processes within the mantle also have the potential to affect the distribution of PGE and Re in mantle samples (Handler *et al.* 1997; Handler & Bennett 1999; Becker *et al.* 2001; Lorand & Alard 2001; Lorand *et al.* 2003, 2004; Büchl *et al.* 2004; Chesley *et al.* 2004; Ionov *et al.* 2006; Ackerman *et al.* 2009; Rudnick & Walker 2009). The peridotites metasomatized by small-volume melts show enrichments in Pt and Pd and elevated $(Pd/Ir)_N$ ratios. In contrast, melt percolation by porous flow at high melt/rock ratios through the mantle can cause breakdown and dissolution of some sulphides and consequent removal of certain PGE from the affected rocks (Lorand & Alard 2001, 2010; Lorand *et al.* 2003, 2004, 2008; Reisberg *et al.* 2004, 2005; Van Acken *et al.* 2008).

Major element data in this study, together with previous petrographic and geochemical data (Xiao *et al.* 2010), show that Beiyan peridotites have experienced pervasive metasomatism (Figs 2–4) and cpx-rich lherzolite and wehrlites are the products of melts interacting with surrounding peridotites in an open system (Xu *et al.* 1996; Xiao *et al.* 2010). Most Beiyan peridotites show broadly flat chondrite-normalized patterns. This is consistent with the residue of low-degree partial melting being affected by the melt process. The total PGE contents decrease greatly with the reduction of MgO of Beiyan peridotites, ranging from lherzolites, cpx-rich lherzolites to wehrlites (Fig. 6a), indicating that melt percolation has evidently caused substantial modification of PGE. Importantly, the two wehrlites (CLB05-80 and CLB05-35) with the lowest MgO contents display extremely low PGE abundances, suggesting that melt flux was sufficiently high to dissolve and remove most of the sulphides. The good positive correlations between PGE and Ir in the Beiyan peridotites (Fig. 5) indicate that a single phase (or several phases behaving in the same way) controls the bulk PGE content during the percolation process. Additionally, the PGE distributions of Beiyan peridotites all display slight Pt depletion. Lorand & Alard (2010) suggested that discrete Pt-rich phases, such as Pt alloys, and not base metal sulphides control the Pt distribution. Therefore, the low Pt concentrations in our samples could be due to the presence of such a Pt-rich phase, which breaks down during melt percolation.

The record of melt percolation in Os isotope compositions

The Re–Os system has been considered to be a reliable means for model age determination of melting events in the mantle because Re behaves moderately incompatibly and Os compatibly during partial melting (Walker *et al.* 1989). Partial melting lowers the Re/Os ratios with increase in the melt portion and therefore reduces the growth of $^{187}Os/^{188}Os$ with time. Also, the high Os contents of xenoliths make them impervious to contamination by host magmas or trapped metasomatic melts (Handler

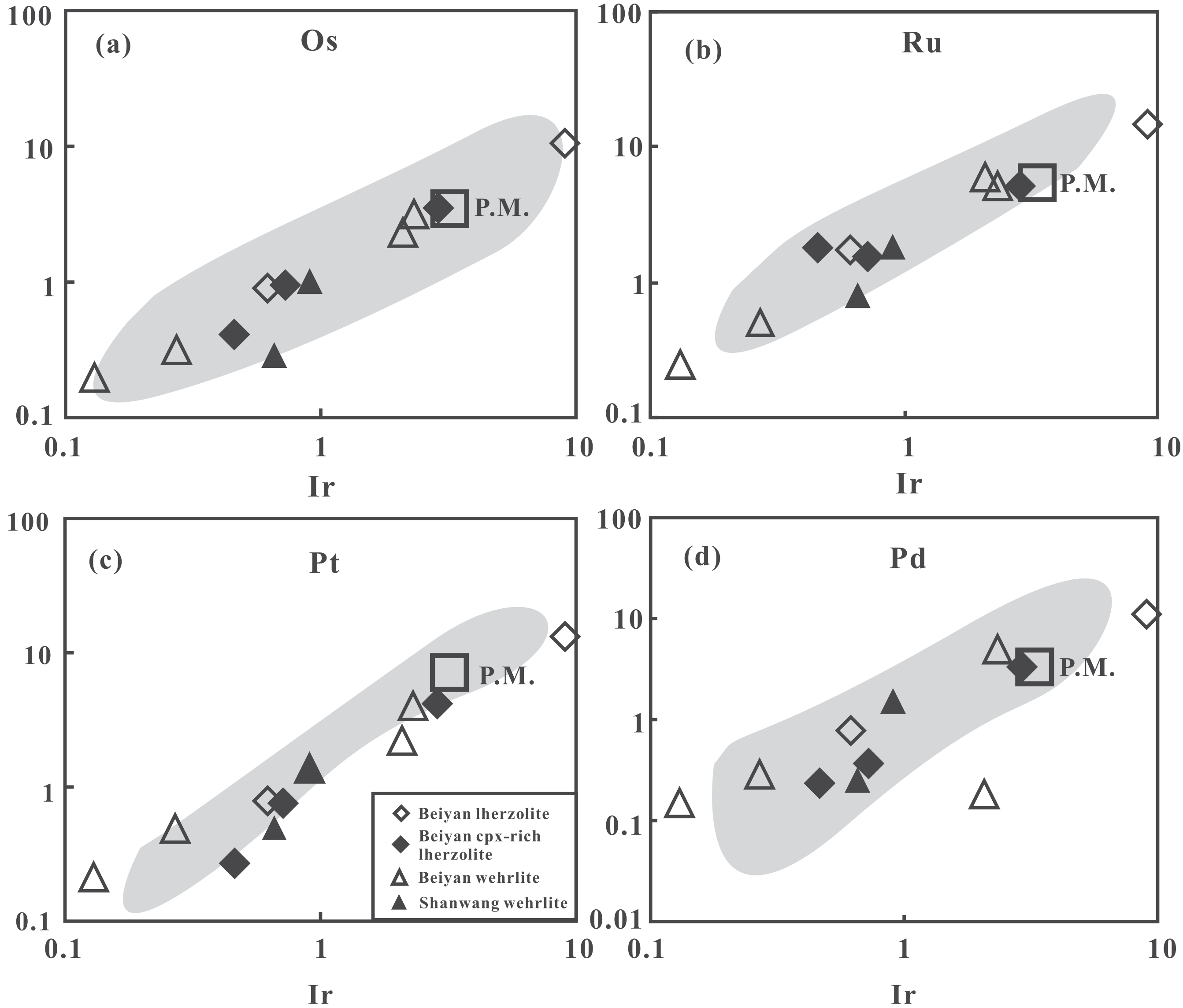

Fig. 5. Bivariate PGE abundance plots. The shaded field indicates data for Shanwang, Nüshan and Yitong lherzolites (Chu *et al.* 2009; Liu *et al.* 2010; Zhou *et al.* 2010). P.M., primitive mantle (McDonough & Sun 1995).

et al. 1997; Olive *et al.* 1997). Many recent studies, however, provide evidence that the Re–Os system in mantle peridotites can be variably affected by late-stage melt percolation and metasomatism (Handler *et al.* 1997; Becker *et al.* 2001; Büchl *et al.* 2002, 2004; Lorand *et al.* 2003, 2004, 2008; Chesley *et al.* 2004; Reisberg *et al.* 2005; Ionov *et al.* 2006; Ackerman *et al.* 2009; Lorand & Alard 2010).

The Os isotopic composition of lherzolites and wehrlites from the Beiyan locality varies in a much larger range (0.12167–0.14978) than that observed in peridotites from the NCC in the Cenozoic (Gao *et al.* 2002; Wu *et al.* 2003, 2006; Zhi *et al.* 2007; Zhang *et al.* 2008, 2009*a*; Chu *et al.* 2009; Liu *et al.* 2010; Zhou *et al.* 2010). The high $^{187}Os/^{188}Os$ values in lithospheric mantle, compared with primitive mantle, are unusual worldwide and cannot be solely explained by partial melting, implying the involvement of a radiogenic melt component. Our data (Figs 7 and 8) also suggest that Os no longer behaves compatibly during massive melt percolation. The most likely reason for this is variable removal of Re and Os after the partial melting with the sulphides by melt. Furthermore, $^{187}Os/^{188}Os$ values in the Beiyan xenoliths and other xenoliths from the Tan-Lu fault zone do not show clear correlation with $^{187}Re/^{188}Os$ (Fig. 9b and c) and therefore typical parent–daughter decay cannot be used for age estimates. In addition, the absence of positive correlations between $^{187}Os/^{188}Os$ and melt extraction index (CaO) for the Beiyan suite must, therefore, be attributed to Os mobility and $^{187}Os/^{188}Os$ changes resulting from melt percolation.

Growth and evolution of lithospheric mantle beneath the eastern NCC

Geochemical studies of mantle xenoliths provide an increasingly complex picture of lithospheric mantle growth and evolution. Trace element and Sr–Nd isotopic studies have documented that newly accreted lithospheric mantle was widespread in late Mesozoic–Cenozoic times beneath the eastern NCC (Zhang 2005; Ying *et al.* 2006; Zheng *et al.* 2007; Tang *et al.* 2008;

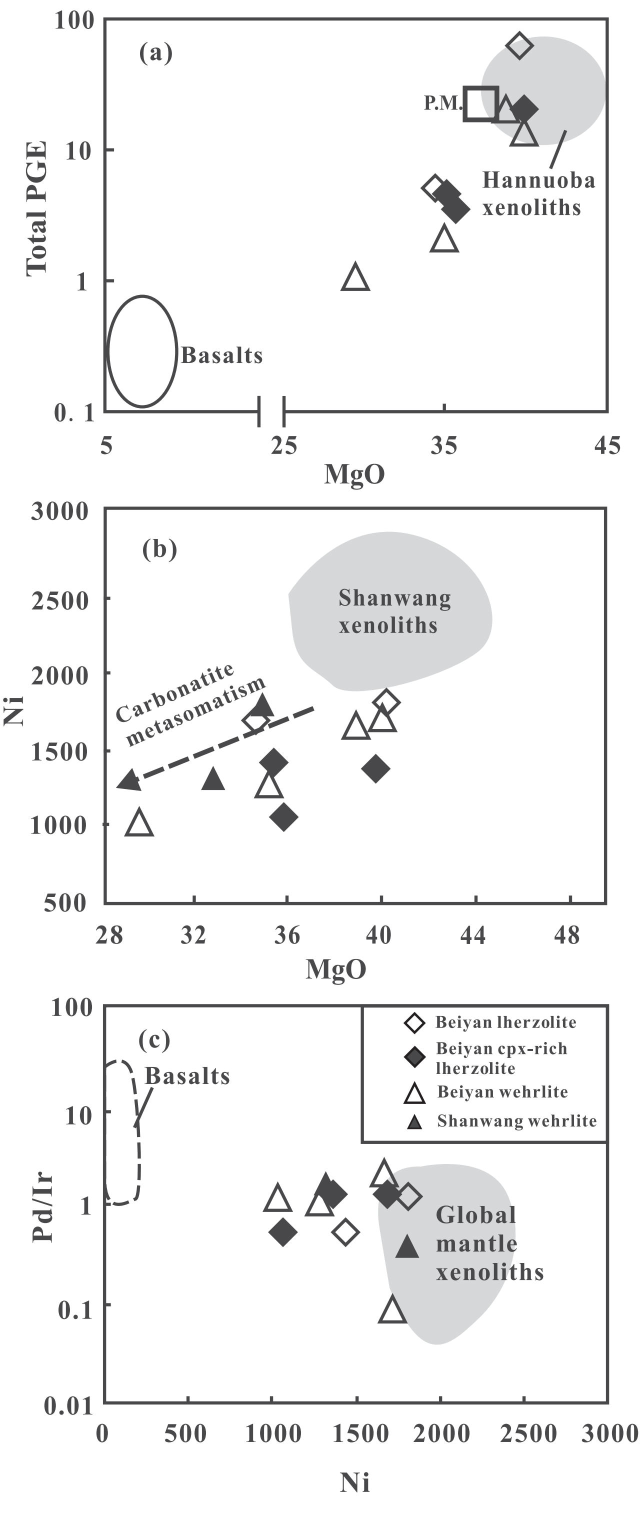

Fig. 6. Plots of (**a**) total PGE abundances v. MgO, (**b**) Ni contents vs. MgO and (**c**) Pd/Ir v. Ni contents for Beiyan peridotites. P.M., primitive mantle (McDonough & Sun 1995). Data sources: Hannuoba, Zhang *et al.* (2007); Shanwang, Chu *et al.* (2009); global mantle xenoliths, McDonald *et al.* (1995); Jining Cenozoic basalts, W.H. Zhang *et al.* (unpublished data). Arrow indicates the effects of predicted carbonatite metasomatism (Handler *et al.* 1997).

Zhang *et al.* 2009*b*, 2010; Xiao *et al.* 2010). Petrographic and geochemical data (Xu *et al.* 1998*a*, 2000; Ying *et al.* 2006; Zheng *et al.* 2007; Tang *et al.* 2008; Zhang *et al.* 2009*b*, 2010; Liu *et al.* 2010; Xiao *et al.* 2010; Zhou *et al.* 2010) show that the lithospheric mantle beneath the eastern NCC has experienced pervasive metasomatism, especially beneath the Tan-Lu fault zone and the Taihang Mountains. This comprehensive chemical and isotope dataset allows us to estimate the possible effects of the metasomatism on the Re–Os system in the eastern NCC mantle, and thus to constrain the origin of Os isotope heterogeneity and the evolution of lithospheric mantle on a regional scale.

The newly accreted lithospheric mantle beneath the eastern NCC experienced low-degree partial melting (<10%) (Zheng *et al.* 1998; Ying *et al.* 2006; Zhang *et al.* 2009*b*). Lherzolites from Kuandian, Penglai and Qixia east to the Tan-Lu fault zone (Fig. 1a) have subchondritic and chondritic $^{187}Os/^{188}Os$ ratios with few suprachondritic values (Fig. 9a) (Gao *et al.* 2002; Wu *et al.* 2003, 2006; Chu *et al.* 2009). The subchondritic $^{187}Os/^{188}Os$ ratios in the peridotites could be explained by ancient partial melting processes. The Os isotopic compositions of the Kuandian and Qixia lherzolites increase with the decrease of Os concentrations, although the trend seems somewhat scattered (Fig. 10a). Figure 8a shows that Os abundances also decrease, accompanied by a decrease in MgO values. These may suggest that Os dissolved and mobilized together with the dissolution of sulphides by melt. Therefore, partial melting cannot explain the mobile Os element and suprachondritic $^{187}Os/^{188}Os$ value observed in these xenoliths. The variable $^{187}Os/^{188}Os$ ratios of lherzolites from these localities may have experienced a younger, spatially restricted reaction with a radiogenic melt after partial melting. Additionally, the Os contents of Penglai lherzolites are very low (most <1 ppb) and show no variation with the increase of $^{187}Os/^{188}Os$ value and the decrease of MgO. The Penglai basalts erupted in the Neogene (5.7–4.2 Ma, Liu 1999) are the youngest volcanism among these localities, suggesting that the metasomatism event must have occurred before 5 Ma.

The lithospheric mantle beneath the Tan-Lu fault zone is different from that away from the Tan-Lu fault zone. The wehrlite xenoliths occur only in the Tan-Lu fault zone (Zheng *et al.* 1998; Chu *et al.* 2009; Liu *et al.* 2010; Xiao *et al.* 2010; Zhou *et al.* 2010) and were formed by interaction between percolating melt and mantle lherzolite (Xiao *et al.* 2010). In addition, most of the lherzolites and wehrlites from the Tan-Lu fault zone have chondritic or suprachondritic Os isotopic compositions (Fig. 9b and c). The $^{187}Os/^{188}Os$ ratios of some peridotites are higher than those of primitive mantle, implying the involvement of a radiogenic melt component. This suggests that the peridotites from the Tan-Lu fault zone could have experienced pervasive melt percolation, which caused a decrease in Os abundances and an increase in Os isotopic ratios of these metasomatized xenoliths. Importantly, the highest $^{187}Os/^{188}Os$ value is shown by one wehrlite (Fig. 9c), which experienced the highest degrees of melt percolation.

Furthermore, the Os concentrations of xenoliths for the eastern NCC are strikingly lower than abundances from spinel peridotite xenoliths worldwide and massif peridotites (Handler *et al.* 1999) (Fig. 11). Thus, the Re–Os system within the mantle from the eastern NCC must have been modified, on a large scale, through melt–rock interaction. Therefore, using Os isotopes to constrain ages of Phanerozoic peridotites is dangerous and the result is highly unreliable. The occurrence of suprachondritic Os isotopic compositions is dominantly in samples from the Tan-Lu fault zone relative to other suites from the eastern NCC, suggesting

Table 3. *Re–Os isotopic compositions of Beiyan peridotites*

Sample	MgO (wt%)	Al_2O_3 (wt%)	Fo	Re (ppb)	Os (ppb)	$^{187}Re/^{188}Os$	$^{187}Os/^{188}Os$	2SD%	γ(Os)	T_{RD} (Ma)	T_{MA} (Ga)
Lherzolite											
CLB05-30	34.5	4.3	89.1	0.0252	0.92	0.133	0.12775	0.22	−1.4	0.26	0.37
CLB05-31	39.6	2.3	90.7	0.5118	10.4	0.237	0.12167	0.07	−6.1	1.09	2.38
Cpx-rich lherzolite											
CLB05-07	35.2	2.4	87.6	0.0002	0.95	0.001	0.12798	0.18	−1.3	0.22	0.23
CLB05-22	40.0	2.1	85.6	0.2096	3.54	0.285	0.12250	0.13	−5.5	0.98	2.82
CLB05-25	35.7	3.7	86.4	0.0577	0.42	0.661	0.13973	0.21	7.8	−1.42	2.60
Wehrlite											
CLB05-01	39.9	1.3	86.9	0.0586	2.32	0.122	0.12453	0.19	−3.9	0.70	0.97
CLB05-35	29.5	4.2	81.7	0.1076	0.19	2.680	0.14978	0.33	15.6	−2.86	0.54
CLB05-46	38.8	2.2	86.8	0.0658	3.21	0.099	0.12620	0.08	−2.6	0.47	0.61
CLB05-80	35.1	3.2	83.3	0.1486	0.31	2.289	0.13124	0.25	1.3	−0.23	0.05

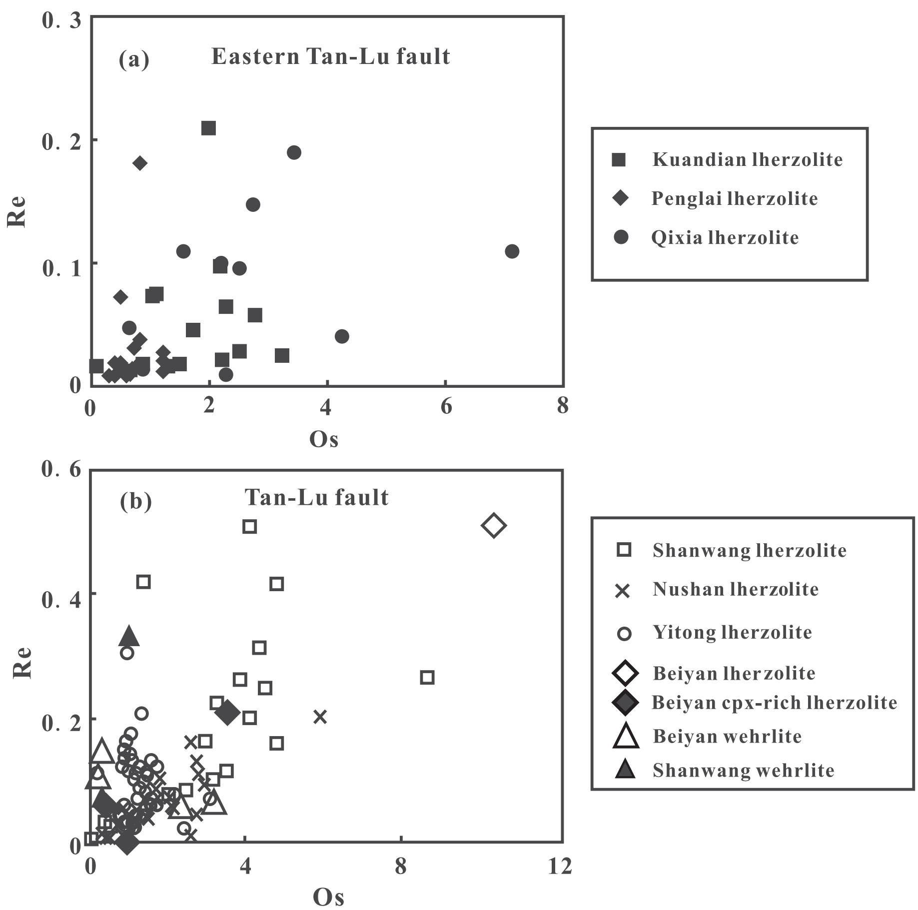

Fig. 7. Variation in Os and Re concentrations for mantle xenoliths in eastern Tan-Lu fault (**a**) and the Tan-Lu fault zone (**b**). The data for peridotites are from Gao *et al.* (2002), Wu *et al.* (2003, 2006), Zhi *et al.* (2007), Chu *et al.* (2009), Liu *et al.* (2010) and Zhou *et al.* (2010).

that the Tan-Lu fault behaved as a conduit for continuous melt ascent. Thus, the newly accreted lithospheric mantle could also be modified through melt–peridotite interaction at a large scale in the eastern NCC.

Nature of the melts

Interaction of the subcontinental mantle with silicate and carbonate melts and/or C–H–O–S fluids is widely documented to affect distribution of the PGE and Re, as well as (more recently) the Re–Os isotopic system (Handler *et al.* 1997; Büchl *et al.* 2004; Van Acken *et al.* 2008; Ackerman *et al.* 2009). The addition of radiogenic Os and also Re from silicate melts migrating in peridotites was suggested by a number of studies (Becker *et al.* 2001; Büchl *et al.* 2002, 2004; Pearson *et al.* 2004; Van Acken *et al.* 2008; Ackerman *et al.* 2009). The different stages of the melt–rock reaction process could also generate contrasting PGE systematics. These latter were controlled by sulphide modal proportions (Cu–Ni sulphides/Mss), silicate melt compositions and melt–rock ratios (Lorand *et al.* 2003).

The abnormally low total PGE contents of Beiyan peridotites can be explained by the pervasive silicate melt percolation that affected the subcontinental lithospheric mantle beneath this locality, shortly before emplacement into host lavas. Because of their low S contents (e.g. Ionov *et al.* 1992), these melts certainly have the potential to dissolve intergranular sulphides

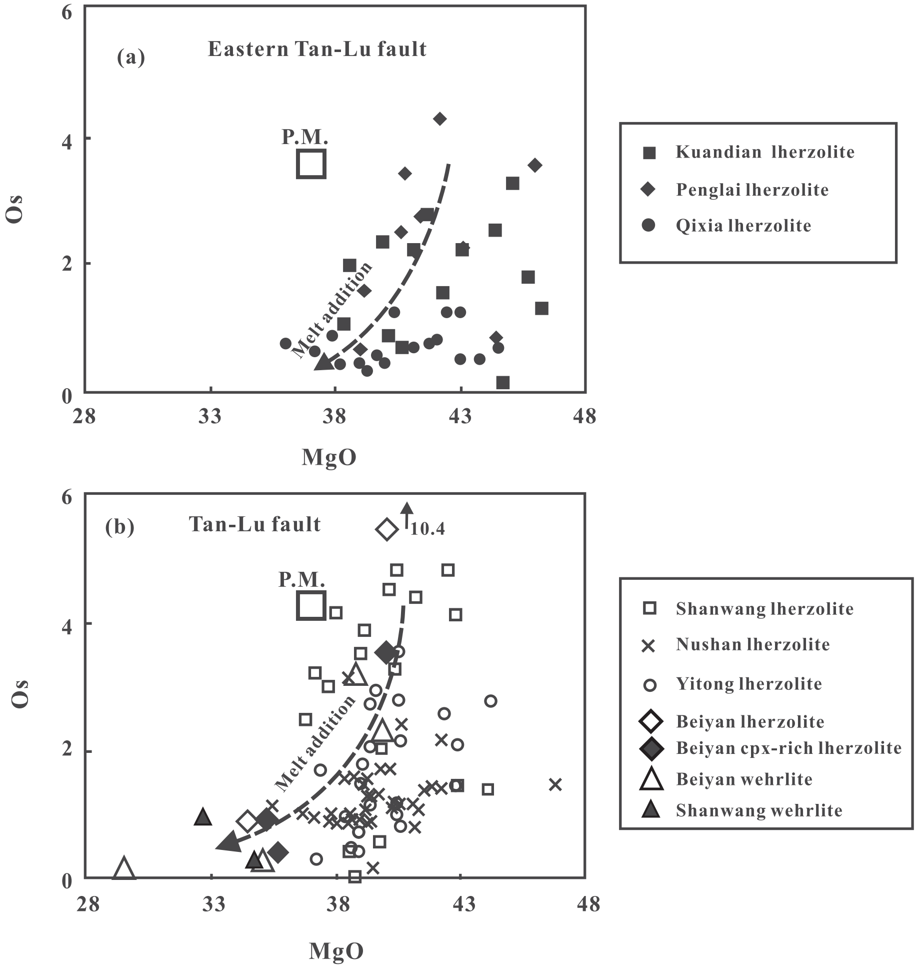

Fig. 8. Variation of Os concentration with MgO for mantle xenoliths in eastern Tan-Lu fault (**a**) and the Tan-Lu fault zone (**b**). The data for peridotites are from Gao *et al.* (2002), Wu *et al.* (2003, 2006), Zhi *et al.* (2007), Chu *et al.* (2009), Liu *et al.* (2010) and Zhou *et al.* (2010).

from the peridotites. On the other hand, young abyssal peridotites, widely believed to be derived from the convecting sub-oceanic mantle, display mostly subchondritic $^{187}Os/^{188}Os$ with a mean value near 0.125 (Martin 1991; Snow & Reisberg 1995; Brandon *et al.* 2000; Alard *et al.* 2005). In contrast to abyssal peridotites, young MORB are characterized by a range of chondritic to moderately suprachondritic $^{187}Os/^{188}Os$ (0.127–0.16) compositions (Martin 1991; Schiano *et al.* 1997; Alard *et al.* 2005; Escrig *et al.* 2005). The suprachondritic Os isotopic ratios and depleted Sr–Nd isotopic compositions (Xiao *et al.* 2010) of Beiyan peridotites also imply that the reactant melt was silicate melt mainly derived from an upwelling of the asthenosphere. However, two wehrlites (CLB05-35 and CLB05-80) have evidently high $^{187}Os/^{188}Os$ ratios that are different from those for other peridotites from Beiyan and the eastern NCC (Fig. 9c). The values of compatible element Ni relative to PGE for Beiyan peridotites are much less than those of basalt-hosted xenoliths of the eastern NCC and the Ni contents for wehrlites have a decreasing trend with MgO (Fig. 6b). The very low Ni content in wehrlites is caused by dilution by the addition of other metasomatic components (Handler *et al.* 1997). The melt may be carbonatitic silicate melt characterized by high percentage of cpx, low Ni and formation of wehrlite. Thus, the Os isotopic heterogeneity and the distribution of PGE observed in Beiyan peridotites appears to be the result of sulphide dissolution and addition of radiogenic Os during melt percolation related to the upwelling of the asthenosphere.

Conclusions

We can draw the following primary conclusions from the above observations.

(1) Beiyan peridotites dominantly have low and variable PGE abundances with the highest MgO lherzolite possessing PGE contents slightly higher than the primitive mantle. The total PGE concentrations generally decrease from lherzolites to highly fertile cpx-rich lherzolites and wehrlites, probably because melt influx was sufficiently high to dissolve and remove most of the sulphides. This study further confirms the conclusion of previous petrological and geochemical studies that pervasive melt percolation affected all these xenoliths.

(2) Beiyan xenoliths show a large variation in $^{187}Os/^{188}Os$ isotopic compositions from chondritic to suprachondritic in lherzolites, cpx-rich lherzolites and wehrlites. This variation is larger than that for peridotites from other xenolith suites in the eastern NCC. Suprachondritic $^{187}Os/^{188}Os$ ratios necessitate the addition of radiogenic Os during melt percolation. Extremely low Os contents in peridotites from the eastern NCC relatively to spinel peridotites worldwide suggest that lowering of Os could also be related to melt percolation.

(3) The wehrlites apparently enriched in CaO relative to the lherzolites have exceedingly low PGE concentrations and high $^{187}Os/^{188}Os$ ratios, probably resulting from the massive flux of carbonatitic silicate melt into the lithosphere.

(4) The Re–Os system within the mantle of the eastern NCC

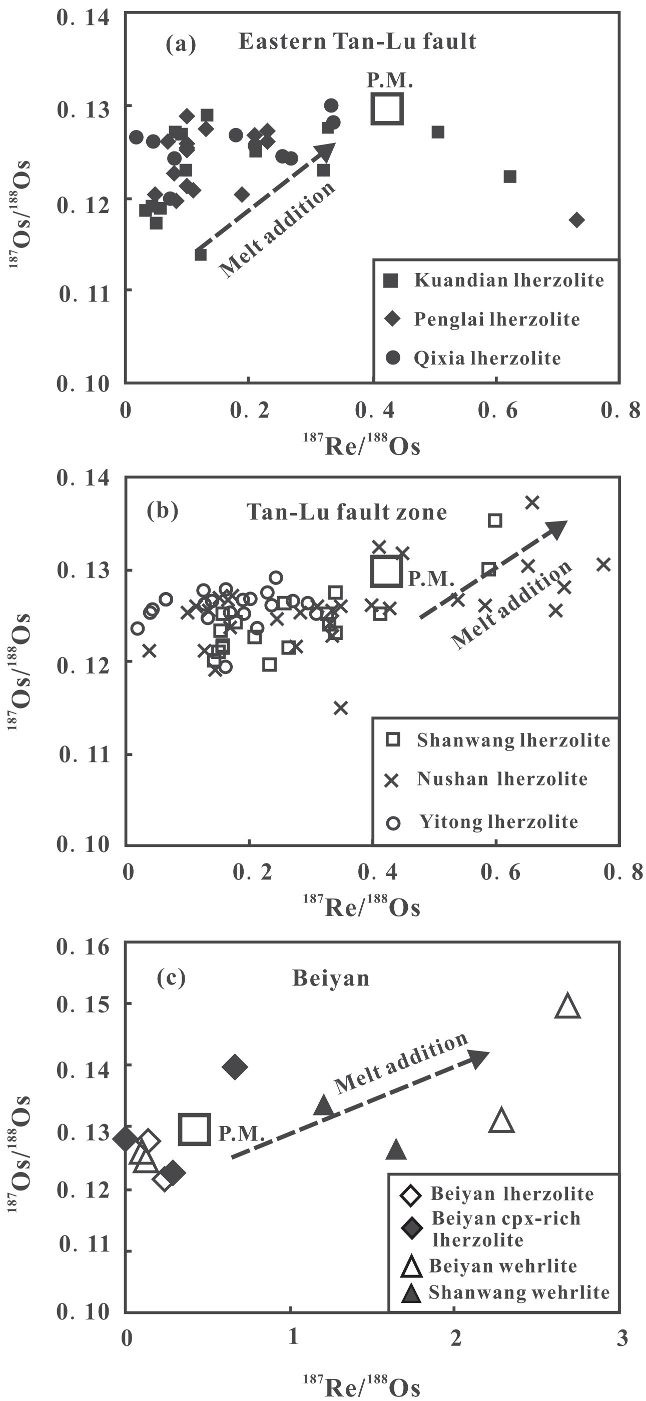

Fig. 9. Plots of $^{187}Os/^{188}Os$ v. $^{187}Re/^{188}Os$ for mantle xenoliths in the eastern Tan-Lu fault (**a**), the Tan-Lu fault zone (**b**) and Beiyan peridotites (**c**). P.M., primitive mantle (Meisel *et al.* 2001). The data for peridotites are from Gao *et al.* (2002), Wu *et al.* (2003, 2006), Zhi *et al.* (2007), Chu *et al.* (2009), Liu *et al.* (2010) and Zhou *et al.* (2010).

may have been modified, on a large scale, through the process of melt–rock interaction. The high enrichment of radiogenic Os isotope in peridotites within the Tan-Lu fault zone relative to those away from it indicates that the Tan-Lu fault zone played an important role as a melt infiltrating channel in the radiogenic Os enrichment induced by the melt percolation, that is, in the evolution of the lithospheric mantle beneath the eastern NCC.

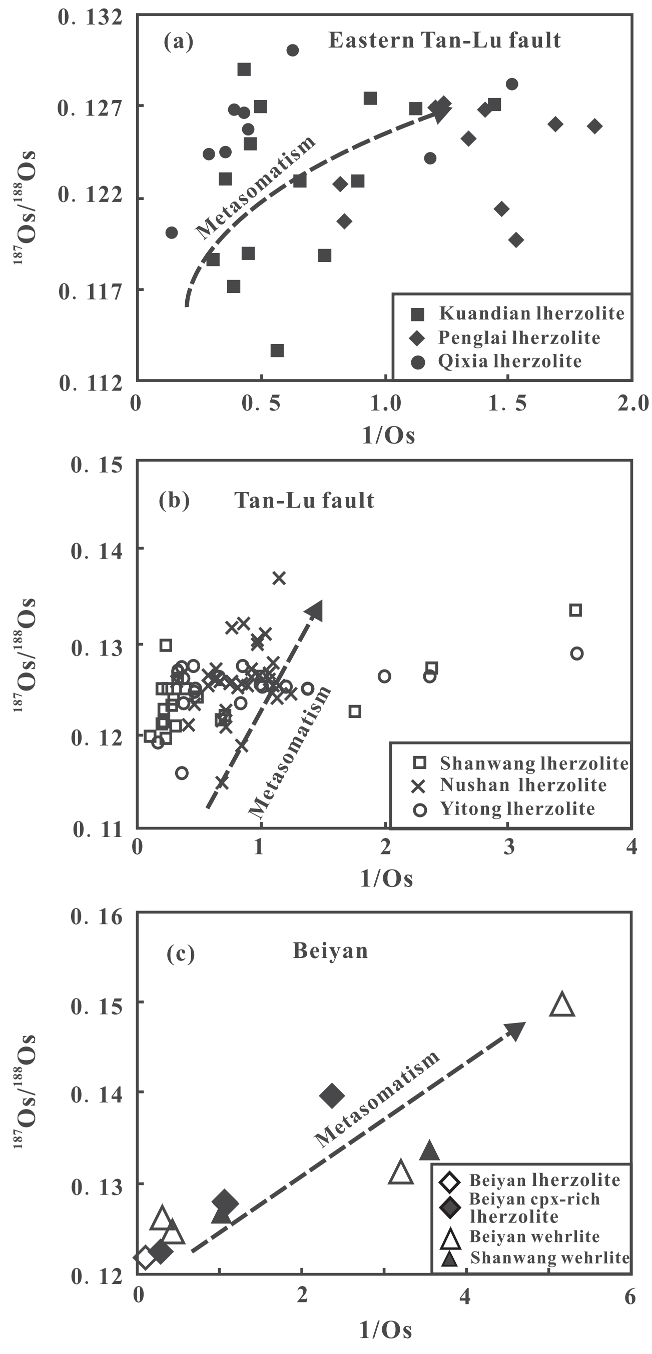

Fig. 10. Variation of $^{187}Os/^{188}Os$ with 1/Os for mantle xenoliths in the eastern Tan-Lu fault (**a**), the Tan-Lu fault zone (**b**) and Beiyan peridotites (**c**). The data for peridotites are from Gao *et al.* (2002), Wu *et al.* (2003, 2006), Zhi *et al.* (2007), Chu *et al.* (2009), Liu *et al.* (2010) and Zhou *et al.* (2010).

The authors would like to thank He Li and Zhuyi Chu for their assistance with major element and Os analyses at the Institute of Geology and Geophysics, Chinese Academy of Sciences. We are also indebted to Yali Sun for her assistance with determination of PGE concentrations and the Os measurement procedures at Guangzhou Institute of Geochemistry, Chinese Academy of Sciences. This research was financially supported by the Nature Science Foundation of China (grants 90714008, 40973012 and 91014007) and a project of the State Key Laboratory of Lithospheric Evolution, Institute of Geology and Geophysics, Chinese Academy of Sciences (Zhuan 1008). We thank S. C. Sherlock and an anonymous

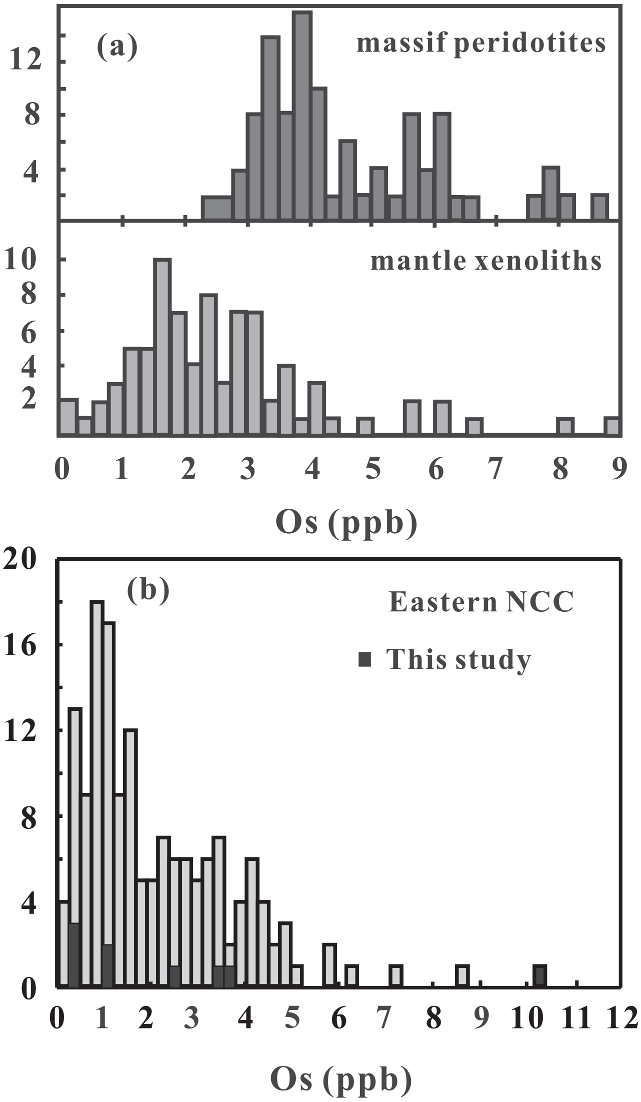

Fig. 11. Histograms of Os abundance data for the eastern NCC peridotites compared with global xenoliths and massif peridotites from the literature. Data for xenoliths and massif peridotites are from Handler *et al.* (1999), Pearson *et al.* (2004), Becker *et al.* (2006), Lorand & Alard (2010) and Fischer-Gödde *et al.* (2011); data for eastern NCC are from Gao *et al.* (2002), Wu *et al.* (2003, 2006), Zhi *et al.* (2007), Chu *et al.* (2009), Liu *et al.* (2010), Zhou *et al.* (2010) and this study.

reviewer for their constructive reviews, which have greatly improved the quality of the paper.

References

Ackerman, L., Walker, R.J., Puchtel, I.S., Pitcher, L., Jelínek, E. & Strnad, L. 2009. Effects of melt percolation on highly siderophile elements and Os isotopes in subcontinental lithospheric mantle: A study of the upper mantle profile beneath Central Europe. *Geochimica et Cosmochimica Acta*, **73**, 2400–2414.

Alard, O., Griffin, W.L., Lorand, J.P., Jackson, S.E. & O'Reilly, S.Y. 2000. Non-chondritic distribution of the highly siderophile elements in mantle sulphides. *Nature*, **407**, 891–894.

Alard, O., Luguet, A., et al. 2005. *In situ* Os isotopes in abyssal peridotites bridge the isotopic gap between MORBs and their source mantle. *Nature*, **436**, 1005–1008.

Anders, E. & Grevesse, N. 1989. Abundances of the elements: Meteoritic and solar. *Geochimica et Cosmochimica Acta*, **53**, 197–214.

Becker, H., Shirey, S.B. & Carlson, R.W. 2001. Effects of melt percolation on the Re–Os systematics of peridotites from a Paleozoic convergent plate margin. *Earth and Planetary Science Letters*, **188**, 107–121.

Becker, H., Horan, M.F., Walker, R.J., Gao, S., Lorand, J.P. & Rudnick, R.L. 2006. Highly siderophile element composition of the Earth's primitive upper mantle: Constraints from new data on peridotite massifs and xenoliths. *Geochimica et Cosmochimica Acta*, **70**, 4528–4550.

Bedini, R.M. & Bodinier, J.L. 1999. Distribution of incompatible trace elements between the constituents of spinel peridotite xenoliths: ICP-MS data from the East African rift. *Geochimica et Cosmochimica Acta*, **63**, 3883–3900.

Bedini, R.M., Bodinier, J.L., Dautria, J.M. & Morten, L. 1997. Evolution of LILE-enriched small melt fractions in the lithospheric mantle: a case study from the East African Rift. *Earth and Planetary Science Letters*, **153**, 67–83.

Bockrath, C., Ballhaus, C. & Holzheid, A. 2004. Fractionation of the platinum-group elements during mantle melting. *Science*, **305**, 1951.

Boyd, F.R. 1989. Compositional distinction between oceanic and cratonic lithosphere. *Earth and Planetary Science Letters*, **96**, 15–26.

Brandon, A.D., Snow, J.E., Walker, R.J., Morgan, J.W. & Mock, T.D. 2000. $^{190}Pt–^{186}Os$ and $^{187}Re–^{187}Os$ systematics of abyssal peridotites. *Earth and Planetary Science Letters*, **177**, 319–335.

Büchl, A., Brugmann, G., Batanova, V.G., Munker, C. & Hofmann, A.W. 2002. Melt percolation monitored by Os isotopes and HSE abundances: A case study from the mantle section of the Troodos Ophiolite. *Earth and Planetary Science Letters*, **204**, 385–402.

Büchl, A., Brugmann, G.E., Batanova, V.G. & Hofmann, A.W. 2004. Os mobilization during melt percolation: The evolution of Os isotope heterogeneities in the mantle sequence of the Troodos ophiolite, Cyprus. *Geochimica et Cosmochimica Acta*, **68**, 3397–3408.

Chesley, J., Righter, K. & Ruiz, J. 2004. Large-scale mantle metasomatism: A Re–Os perspective. *Earth and Planetary Science Letters*, **219**, 49–60.

Chu, Z.Y., Wu, F.Y., et al. 2009. Temporal evolution of the lithospheric mantle beneath the Eastern North China Craton. *Journal of Petrology*, **50**, 1857–1898.

Downes, H. 2001. Formation and modification of the shallow sub-continental lithospheric mantle: a review of geochemical evidence from ultramafic xenolith suites and tectonically emplaced ultramafic massifs of western and central Europe. *Journal of Petrology*, **42**, 233–250.

Escrig, S., Schiano, P., Schilling, J.G. & Allègre, C. 2005. Rhenium–osmium isotope systematics in MORB from the Southern Mid-Atlantic Ridge (40°–50°S). *Earth and Planetary Science Letters*, **235**, 528–548.

Fan, W.M., Zhang, H.F., Baker, J., Jarvis, K.E., Mason, P.R.D. & Menzies, M.A. 2000. On and off the North China Craton: Where is the Archaean keel? *Journal of Petrology*, **41**, 933–950.

Fischer-Gödde, M., Becker, H. & Wombacher, F. 2010. Rhodium, gold and other highly siderophile element abundances in chondritic meteorites. *Geochimica et Cosmochimica Acta*, **74**, 356–379.

Fischer-Gödde, M., Becker, H. & Wombacher, F. 2011. Rhodium, gold and other highly siderophile elements in orogenic peridotites and peridotite xenoliths. *Chemical Geology*, **280**, 365–383.

Gao, S., Rudnick, R.L., Carlson, R.W., McDonough, W.F. & Liu, Y.S. 2002. Re–Os evidence for replacement of ancient mantle lithosphere beneath the North China craton. *Earth and Planetary Science Letters*, **198**, 307–322.

Griffin, W.L., Andi, Z., O'Reilly, S.Y. & Ryan, C.G. 1998. Phanerozoic evolution of the lithosphere beneath the Sino-Korean Craton. *In*: Flower, M.F.J., Chung, S.L., Lo, C.H. & Lee, T.Y. (eds) *Mantle Dynamics and Plate Interactions in East Asia*. American Geophysical Union, Geodynamics Series, **27**, 107–126.

Griffin, W.L., O'Reilly, S.Y. & Ryan, C.G. 1999. The composition and origin of sub-continental lithospheric mantle. *In:* Fei, Y., Bertka, C.M. & Mysen, B.O. (eds) *Mantle Petrology: Field Observations and High-pressure Experimentation: a Tribute to Francis R (Joe) Boyd*. The Geochemical Society, Houston, 13–46.

Handler, M.R. & Bennett, V.C. 1999. Behaviour of Platinum-group elements in the subcontinental mantle of eastern Australia during variable metasomatism and melt depletion. *Geochimica et Cosmochimica Acta*, **63**, 3597–3618.

Handler, M.R., Bennett, V.C. & Esat, T.M. 1997. The persistence of off-cratonic lithospheric mantle: Os isotopic systematics of variably metasomatised southeast Australian xenoliths. *Earth and Planetary Science Letters*, **151**, 61–75.

Handler, M.R., Bennett, V.C. & Dreibus, G. 1999. Evidence from correlated Ir/Os and Cu/S for late-stage Os mobility in peridotite xenoliths: Implications for Re–Os systematics. *Geology*, **27**, 75–78.

Harris, J.W., Duncan, D.J., Zhang, F., Miao, Q. & Zhu, Y. 1994. The physical characteristics and syngenetic inclusion geochemistry of diamonds from Pipe 50, Liaoning province, People's Republic of China. *In*: Meyer, H.O.A., Leonardos, O.H. (eds) *Diamonds: Characterisation, Genesis and Explora-*

tion, Vol. 2. CPRM (Brazil), Special Publication, **1A,** 106–115.

Ionov, D., Savoyant, L. & Dupuy, C. 1992. Application of the ICP-MS technique to trace element analysis of peridotites and their minerals. *Geostandards Newsletter*, **16**, 311–315.

Ionov, D.A., Shirey, S.B., Weis, D. & Brugmann, G. 2006. Os–Hf–Sr–Nd isotope and PGE systematics of spinel peridotite xenoliths from Tok, SE Siberian craton: Effects of pervasive metasomatism in shallow refractory mantle. *Earth and Planetary Science Letters*, **241**, 47–64.

Kelemen, P.B., Hart, S.R. & Bernstein, S. 1998. Silica enrichment in the continental upper mantle via melt/rock reaction. *Earth and Planetary Science Letters*, **164**, 387–406.

Lee, C.T. 2002. Platinum-group element geochemistry of peridotite xenoliths from the Sierra Nevada and the Basin and Range, California. *Geochimica et Cosmochimica Acta*, **66**, 3987–4005.

Lee, C.T. & Rudnick, R.L. 1999. Compositionally stratified cratonic lithosphere: Petrology and geochemistry of peridotite xenoliths the Labait volcano, Tanzania. *In:* Gurney, J.J., Gurney, J.L. & Pascoe, M.D. (eds) *Proceedings of the 7th International Kimberlite Conference*. Red Roof Design, Cape Town, 503–521.

Liu, D.Y., Nutman, A.P., Compston, W., Wu, J.S. & Shen, Q.H. 1992. Remnants of 3800 Ma crust in the Chinese part of the Sino-Korean Craton. *Geology*, **20**, 1–20.

Liu, J.G. 1999. *Active Volcanoes in China*. Science Press, Beijing [in Chinese].

Liu, Z.C., Wu, F.C., Chu, Z.Y. & Xu, X.S. 2010. Isotopic compositions of the peridotitic xenoliths from the Nushan, Anhui Province: Constraints on the age of subcontinental lithospheric mantle beneath the East China. *Acta Petrologica Sinica*, **26**, 1217–1240 [in Chinese with English abstract].

Lorand, J.P. & Alard, O. 2001. Platinum-group element abundances in the upper mantle: New constraints from *in situ* and whole-rock analyses of Massif Central xenoliths (France). *Geochimica et Cosmochimica Acta*, **65**, 2789–2806.

Lorand, J.P. & Alard, O. 2010. Platinum-group element micronuggets and refertilization process in Lherz orogenic peridotite (northeastern Pyrenees, France). *Earth and Planetary Science Letters*, **289**, 298–310.

Lorand, J.P., Keays, R.R. & Bodinier, J.L. 1993. Copper and noble-metal enrichments across the lithosphere–asthenosphere boundary of mantle diapirs—evidence from the Lanzo Lherzolite Massif. *Journal of Petrology*, **34**, 1111–1140.

Lorand, J.P., Pattou, L. & Gros, M. 1999. Fractionation of platinum-group elements and gold in the upper mantle: A detailed study in Pyrenean orogenic lherzolites. *Journal of Petrology*, **40**, 957–981.

Lorand, J.P., Reisberg, L. & Bedini, R.M. 2003. Platinum-group elements and melt percolation processes in Sidamo spinel peridotite xenoliths, Ethiopia, East African Rift. *Chemical Geology*, **196**, 57–75.

Lorand, J.P., Delpech, G., Gregoire, M., Moine, B., O'Reilly, S.Y. & Cottin, J.Y. 2004. Platinum-group elements and the multistage metasomatic history of Kerguelen lithospheric mantle (South Indian Ocean). *Chemical Geology*, **208**, 195–215.

Lorand, J.P., Luguet, A., Alard, O., Bezos, A. & Meisel, T. 2008. Abundance and distribution of platinum-group elements in orogenic lherzolites: A case study in a Fontete Rouge lherzolite. *Chemical Geology*, **248**, 174–194.

Luguet, A., Lorand, J.P., Alard, O. & Cottin, J.Y. 2004. A multi-technique study of platinum group element systematic in some Ligurian ophiolitic peridotites, Italy. *Chemical Geology*, **208**, 175–194.

Luguet, A., Shirey, S.B., Lorand, J.P., Horan, M.F. & Carlson, R.W. 2007. Residual platinum-group minerals from highly depleted harzburgites of the Lherz massif (France) and their role in HSE fractionation of the mantle. *Geochimica et Cosmochimica Acta*, **71**, 3082–3097.

Martin, C.E. 1991. Osmium isotopic characteristics of mantle-derived rocks. *Geochimica et Cosmochimica Acta*, **55**, 1421–1434.

McDonald, I., De Wit, M.J., Smith, C.B., Bizzi, L.A. & Viljoen, K.S. 1995. The geochemistry of the platinum-group elements in Brazilian and southern African kimberlites. *Geochimica et Cosmochimica Acta*, **59**, 2883–2903.

McDonough, W.F. & Sun, S.S. 1995. The composition of the Earth. *Chemical Geology*, **120**, 223–253.

Meisel, T., Walker, R.J., Irving, A.J. & Lorand, J.P. 2001. Osmium isotopic compositions of mantle xenoliths: A global perspective. *Geochimica et Cosmochimica Acta*, **65**, 1311–1323.

Menzies, M., Xu, Y.G., Zhang, H.F. & Fan, W.M. 2007. Integration of geology, geophysics and geochemistry: A key to understanding the North China Craton. *Lithos*, **96**, 1–21.

Menzies, M.A., Fan, W.M. & Zhang, M. 1993. Palaeozoic and Cenozoic lithoprobes and the loss of 120 km of Archaean lithosphere, Sino-Korean craton, China. *In:* Prichard, H.M., Alabaster, T., Harris, N.B.W. & Neary, C.R. (eds) *Magmatic Processes and Plate Tectonics*. Geological Society, London, Special Publications, **76**, 71–81.

Meyer, H.O.A., Zhang, A. & Milledge, H.J. 1994. Diamonds and Inclusions in Diamonds from Chinese Kimberlites. *In:* Meyer, H.O.A., Leonardos, O.H. (eds) *Diamonds: Characterisation, Genesis and Exploration, Vol. 2.* CPRM (Brazil), Special Publication, **1A,** 98–105.

Mitchell, R.H. & Keays, R.R. 1981. Abundance and distribution of gold, palladium and iridium in some spinel and garnet lherzolites: Implications for the nature and origin of precious metal-rich intergranular components in the upper mantle. *Geochimica et Cosmochimica Acta*, **45**, 2425–2433.

Morgan, J. 1986. Ultramafic xenoliths: clues to Earth's late accretionary history. *Journal of Geophysical Research*, **91**, article number 12375.

Morgan, J.W., Walker, R.J., Brandon, A.D. & Horan, M.F. 2001. Siderophile elements in Earth's upper mantle and lunar breccias: Data synthesis suggests manifestations of the same late influx. *Meteoritics and Planetary Science*, **36**, 1257–1276.

Olive, V., Ellam, R.M. & Harte, B. 1997. A Re–Os isotope study of ultramafic xenoliths from the Matsoku kimberlite. *Earth and Planetary Science Letters*, **150**, 129–140.

Pattou, L., Lorand, J.P. & Gros, M. 1996. Non-chondritic platinum-group element ratios in the Earth's mantle. *Nature*, **379**, 712–715.

Pearson, D.G., Irvine, G.J., Ionov, D.A., Boyd, F.R. & Dreibus, G.E. 2004. Re–Os isotope systematics and platinum group element fractionation during mantle melt extraction: a study of massif and xenolith peridotite suites. *Chemical Geology*, **208**, 29–59.

Rehkämper, M., Halliday, A.N., Barfod, D. & Fitton, J.G. 1997. Platinum-group element abundance patterns in different mantle environments. *Science*, **278**, 1595–1598.

Rehkämper, M., Halliday, A.N., Alt, J., Fitton, J.G., Zipfel, J. & Takazawa, E. 1999. Non-chondritic platinum-group element ratios in oceanic mantle lithosphere: petrogenetic signature of melt percolation? *Earth and Planetary Science Letters*, **172**, 65–81.

Reisberg, L., Ohnenstetter, M., Alard, O. & Lorand, J.P. 2004. Highly siderophile element behavior in high temperature processes—Preface. *Chemical Geology*, **208**, 1–4.

Reisberg, L., Zhi, X.C., Lorand, J.P., Wagner, C., Peng, Z.C. & Zimmermann, C. 2005. Re–Os and S systematics of spinel peridotite xenoliths from east central China: Evidence for contrasting effects of melt percolation. *Earth and Planetary Science Letters*, **239**, 286–308.

Rudnick, R.L. & Walker, R.J. 2009. Interpreting ages from Re–Os isotopes in peridotites. *Lithos*, **112S**, 1083–1095.

Rudnick, R.L., Shan, G., Ling, W.L., Liu, Y.S. & McDonough, W.F. 2004. Petrology and geochemistry of spinel peridotite xenoliths from Hannuoba and Qixia, North China craton. *Lithos*, **77**, 609–637.

Schiano, P., Birck, J.L. & Allègre, C.J. 1997. Osmium–strontium–neodymium–lead isotopic covariations in mid-ocean ridge basalt glasses and the heterogeneity of the upper mantle. *Earth and Planetary Science Letters*, **150**, 363–379.

Shirey, S.B. & Walker, R.J. 1998. The Re–Os isotope system in cosmochemistry and high-temperature geochemistry. *Annual Review of Earth and Planetary Sciences*, **26**, 423–500.

Snow, J.E. & Reisberg, L. 1995. Os isotopic systematics of the MORB mantle: results from altered abyssal peridotites. *Earth and Planetary Science Letters*, **133**, 411–421.

Snow, J.E. & Schmidt, G. 1998. Constraints on Earth accretion deduced from noble metals in the oceanic mantle. *Nature*, **391**, 166–169.

Sun, Y.L., Chu, Z.Y., Sun, M. & Xia, X.P. 2009. An improved Fe–Ni sulfide fire assay method for determination of Re, platinum group elements, and Os isotopic ratios by inductively coupled plasma- and negative thermal ionization-mass spectrometry. *Society for Applied Spectroscopy*, **63**, 1232–1237.

Tang, Y.J., Zhang, H.F., Ying, J.F., Zhang, J. & Liu, M.X. 2008. Refertilization of ancient lithospheric mantle beneath the central North China Craton: Evidence from petrology and geochemistry of peridotite xenoliths. *Lithos*, **101**, 435–452.

Van Acken, D., Becker, H. & Walker, R.J. 2008. Refertilization of Jurassic oceanic peridotites from the Tethys Ocean—Implications for the Re–Os systematics of the upper mantle. *Earth and Planetary Science Letters*, **268**, 171–181.

Walker, R., Carlson, R., Shirey, S. & Boyd, F.R. 1989. Os, Sr, Nd, and Pb isotope systematics of southern African peridotite xenoliths: implications for the chemical evolution of subcontinental mantle. *Geochimica et Cosmochimica Acta*, **53**, 1583–1595.

Wu, F.Y., Walker, R.J., Ren, X.W., Sun, D.Y. & Zhou, X.H. 2003. Osmium isotopic constraints on the age of lithospheric mantle beneath northeastern China. *Chemical Geology*, **196**, 107–129.

Wu, F.Y., Walker, R.J., Yang, Y.H., Yuan, H.L. & Yang, J.H. 2006. The chemical–temporal evolution of lithospheric mantle underlying the North China Craton. *Geochimica et Cosmochimica Acta*, **70**, 5013–5034.

Xiao, Y., Zhang, H.F., Fan, W.M., Ying, J.F., Zhang, J., Zhao, X.M. & Su, B.X. 2010. Evolution of lithospheric mantle beneath the Tan-Lu fault zone, eastern North China Craton: Evidence from petrology and geochemistry of peridotite xenoliths. *Lithos*, **117**, 229–246.

Xu, X.S., O'Reilly, S.Y. & Griffin, W.L. 1998*a*. The nature of the Cenozoic lithosphere at Nüshan, Eastern China. *In:* Flower, M.F.J., Chung, S.L., Lo, C.H. & Lee, C.T. (eds) *Mantle Dynamics and Plate Interaction in Eastern Asia*. American Geophysical Union, Geodynamics Series, **27**, 167–195.

Xu, X.S., O'Reilly, S.Y., Griffin, W.L. & Zhou, X.M. 2000. Genesis of young lithospheric mantle in southeastern China: an LAM-ICPMS trace element study. *Journal of Petrology*, **41**, 111–148.

Xu, Y.G. 2001. Thermo-tectonic destruction of the Archaean lithospheric keel beneath the Sino-Korean Craton in China: Evidence, timing and mechanism. *Physics and Chemistry of the Earth, Part A: Solid Earth and Geodesy*, **26**, 747–757.

Xu, Y.G., Mercier, J.C.C., Menzies, M.A., Ross, J.V., Harte, B., Lin, C.Y. & Shi, L.B. 1996. K-rich glass-bearing wehrlite xenoliths from Yitong, northeastern China: Petrological and chemical evidence for mantle metasomatism. *Contributions to Mineralogy and Petrology*, **125**, 406–420.

Xu, Y.G., Orberger, B. & Reeves, S.J. 1998*b*. Fractionation of platinum group elements in upper mantle: evidence from peridotite xenoliths from Wangqing. *Science in China Series D: Earth Sciences*, **41**, 354–361.

Ying, J.F., Zhang, H.F., Kita, N., Morishita, Y. & Shimoda, G. 2006. Nature and evolution of late Cretaceous lithospheric mantle beneath the eastern North China Craton: Constraints from petrology and geochemistry of peridotitic xenoliths from Junan, Shandong Province, China. *Earth and Planetary Science Letters*, **244**, 622–638.

Zhang, H.F. 2005. Transformation of lithospheric mantle through peridotite–melt reaction: A case of Sino-Korean craton. *Earth and Planetary Science Letters*, **237**, 768–780.

Zhang, H.F. & Sun, M. 2002. Geochemistry of Mesozoic basalts and mafic dikes, southeastern north China craton, and tectonic implications. *International Geology Review*, **44**, 370–382.

Zhang, H.F. & Yang, Y.H. 2007. Emplacement age and Sr–Nd–Hf isotopic characteristics of the diamondiferous kimberlites from the eastern North China Craton. *Acta Petrologica Sinica*, **23**, 285–294 [in Chinese with English abstract].

Zhang, H.F., Goldstein, S.L., Zhou, X.H., Sun, M., Zheng, J.P. & Cai, Y. 2008. Evolution of subcontinental lithospheric mantle beneath eastern China: Re–Os isotopic evidence from mantle xenoliths in Paleozoic kimberlites and Mesozoic basalts. *Contributions to Mineralogy and Petrology*, **155**, 271–293.

Zhang, H.F., Goldstein, S.L., Zhou, X.H., Sun, M. & Cai, Y. 2009*a*. Comprehensive refertilization of lithospheric mantle beneath the North China Craton: further Os–Sr–Nd isotopic constraints. *Journal of the Geological Society, London*, **166**, 249–259.

Zhang, H.F., Deloule, E., Tang, J.Y. & Ying, J.F. 2010. Melt/rock interaction in remains of refertilized Archean lithospheric mantle in Jiaodong Peninsula, North China Craton: Li isotopic evidence. *Contributions to Mineralogy and Petrology*, **160**, 261–277.

Zhang, J., Zhang, H.F., Kita, N., Shimoda, G., Morishita, Y., Ying, J.F. & Tang, Y.J. 2009*b*. Secular evolution of the lithospheric mantle beneath the eastern North China craton: evidence from peridotitic xenoliths from Late Cretaceous mafic rocks in the Jiaodong region, east–central China. *International Geology Review*, doi:10.1080/00206810903025090.

Zhang, W.P., Hao, Y. & Yue, K.F. 2007. Studies on enriching law of gold in mantle xenoliths: A case study of eastern China. *Journal of Earth Sciences and Environment*, **29**, 117–119 [in Chinese with English abstract].

Zhao, G.C., Wilde, S.A., Cawood, P.A. & Sun, M. 2001. Archean blocks and their boundaries in the North China Craton: Lithological, geochemical, structural and *P–T* path constraints and tectonic evolution. *Precambrian Research*, **107**, 45–73.

Zheng, J.P., O'Reilly, S.Y., Griffin, W.L., Lu, F.X. & Zhang, M. 1998. Nature and evolution of Cenozoic lithospheric mantle beneath Shandong peninsula, Sino-Korean Craton, eastern China. *International Geology Review*, **40**, 471–499.

Zheng, J.P., O'Reilly, S.Y., Griffin, W.L., Lu, F.X., Zhang, M. & Pearson, N.J. 2001. Relict refractory mantle beneath the eastern North China block: Significance for lithosphere evolution. *Lithos*, **57**, 43–66.

Zheng, J.P., Sun, M., Zhou, M.F. & Robinson, P. 2005. Trace elemental and PGE geochemical constraints of Mesozoic and Cenozoic peridotitic xenoliths on lithospheric evolution of the North China Craton. *Geochimica et Cosmochimica Acta*, **69**, 3401–3418.

Zheng, J.P., Griffin, W.L., O'Reilly, S.Y., Yu, C.M., Zhang, H.F., Pearson, N. & Zhang, M. 2007. Mechanism and timing of lithospheric modification and replacement beneath the eastern North China Craton: Peridotitic xenoliths from the 100 Ma Fuxin basalts and a regional synthesis. *Geochimica et Cosmochimica Acta*, **71**, 5203–5225.

Zhi, X.C., Reisberg, L. & Xu, X.S. 2007. Re–Os geochmistry of mantle peridotite xenoliths from Nushan. *Journal of University of Science and Technology of China*, **37**, 945–952 [in Chinese with English abstract].

Zhou, Q., Wu, F.Y., Chu, Z.Y. & Ge, W.C. 2010. Isotopic compositions of mantle xenoliths and age of the lithospheric mantle in Yitong, Jilin Province. *Acta Petrologica Sinica*, **26**, 1241–1264 [in Chinese with English abstract].

Received 29 June 2010; revised typescript accepted 1 April 2011.
Scientific editing by Sarah Sherlock.